iScience

CellPress
OPEN ACCESS

Article

Tetrapodal textured Janus textiles for accessible menstrual health

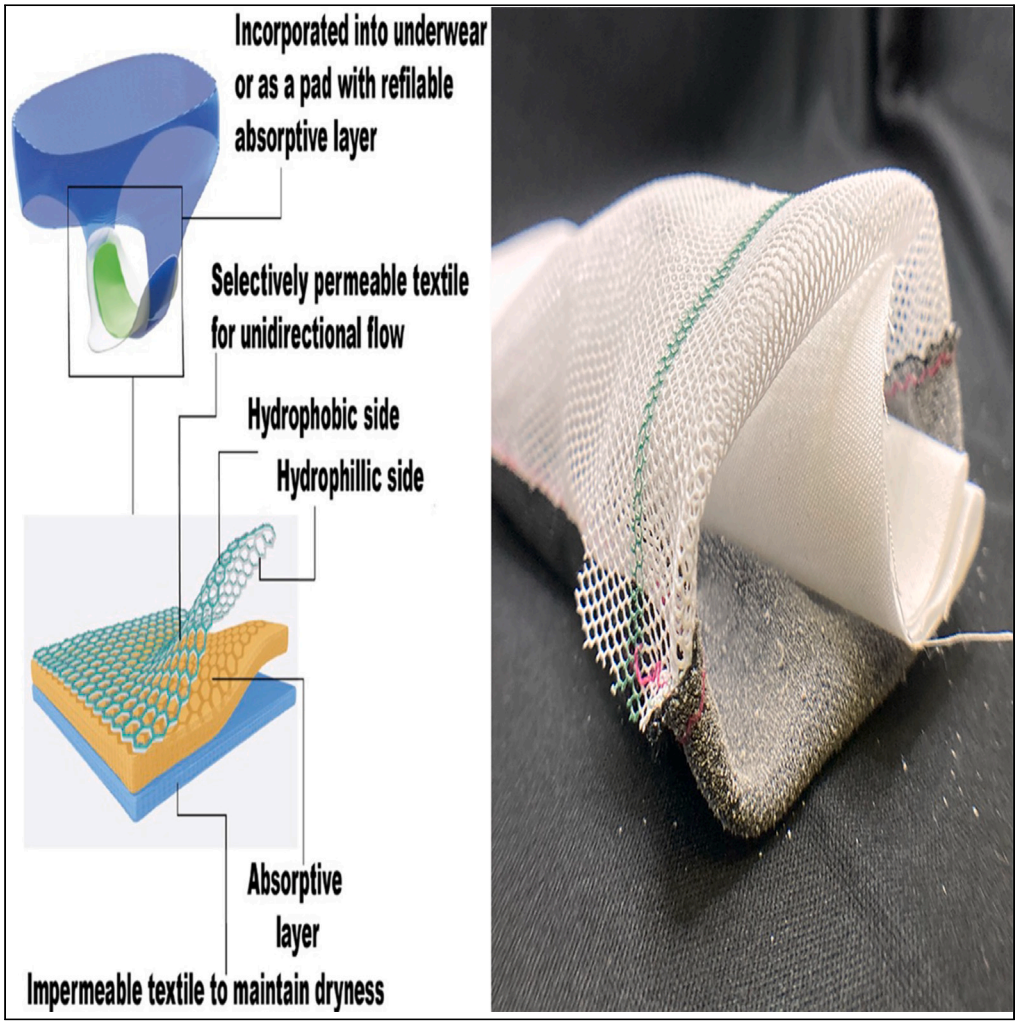

Sarah L. Sanders, Lacey D. Douglas, Tiffany E. Sill, ..., Lei Fang, Rachel D. Davidson, Sarbajit Banerjee

rachelda@udel.edu (R.D.D.)
banerjee@chem.tamu.edu (S.B.)

Highlights

Body-facing "Janus" fabric comprising ZnO tetrapods integrated onto mosquito netting

Unidirectional flow established even under 1 kg of applied weight

Liquid strike-through and wetback tests for saline media and menstrual fluid simulant

Assembled prototype performs comparably to commercial pads under standardized testing

Sanders et al., iScience *26*, 108224
November 17, 2023
https://doi.org/10.1016/j.isci.2023.108224

iScience

CellPress
OPEN ACCESS

Article

Tetrapodal textured Janus textiles for accessible menstrual health

Sarah L. Sanders,[1,2,4] Lacey D. Douglas,[1,2,4] Tiffany E. Sill,[1,2] Kaylyn Stewart,[1,2] Noah Pieniazek,[1,2] Chenxuan Li,[1] Eve Walters,[1,2] Mohammed Al-Hashimi,[3] Lei Fang,[1] Rachel D. Davidson,[1,2,*] and Sarbajit Banerjee[1,2,5,*]

SUMMARY

Menstruating individuals without access to adequate hygiene products often improvise with alternatives that pose health risks and limit their participation in society. We describe here a menstrual hygiene product based on low-cost materials, which are integrated onto fabrics to imbue unidirectional permeability. A body-facing "Janus" fabric top layer comprising ZnO tetrapods spray-coated onto polyester mosquito netting imparts hierarchical texturation, augmenting the micron-scale texturation derived from the weave of the underlying fabric. The asymmetric coating establishes a gradient in wettability, which underpins flash spreading and unidirectional permeability. The hygiene product accommodates a variety of absorptive media, which are sandwiched between the Janus layer and a second outward-facing coated densely woven fabric. An assembled prototype demonstrates outstanding ability to wick saline solutions and a menstrual fluid simulant while outperforming a variety of commercially alternatives. The results demonstrate a versatile menstrual health product that provides a combination of dryness, discretion, washability, and safety.

INTRODUCTION

Several hundred million people between menarche and menopause in low- and middle-income scenarios do not have adequate resources to manage their menstrual health needs, thereby limiting their ability to realize their full potential and placing their physical and mental health at risk. The lack of viable, affordable, safe, sustainable, and discreet menstrual hygiene products is a result of financial constraints, lack of access to clean water, and social constructs.[1–4] Menstruating individuals who do not have access to adequate resources often have to improvise with woefully inadequate alternatives such as tissue, discarded fabrics, rags, newspapers, or leaves.[5] As such, there is an urgent need for a low-cost menstrual hygiene product that provides a combination of dryness, discretion, washability, safety, and ease of fabrication. In this article, we report a surface modification method based on low-cost materials that can readily transform locally sourced textiles into selectively permeable materials that enforce the unidirectional transport of fluids. These coated textiles have been assembled to build multi-layered menstrual hygiene products whose performance has been validated through standardized strike-through and wetback testing.

Absorption products for human hygiene such as menstrual hygiene pads, diapers, and bed pads for urinary incontinence are ubiquitously configured to have three distinct layers, a permeable layer that makes contact with skin, a middle absorption medium, and an impermeable back sheet that serves to contain the absorbed liquid within the absorption media.[6,7] For single-use pads the absorption layer has been the primary focus of research. Considerable attention has been devoted to the development of superabsorbent polymers with still greater capacity.[8,9] However, such engineered polymers can be difficult to source in resource-poor scenarios. Such materials are furthermore inherently single use in nature. Motivated by sustainability concerns, considerable recent attention has focused on the design of single-use pads that supplant absorbent polymers with more biodegradable absorptive mediums such as cellulose. Reusable pads have also started to gain prominence and have claimed considerable market share in recent years. Several commercial products are based on just two layers; an absorbent fabric that faces the body (fleece being a common choice) coupled with a leak-proof outer layer. These multilayered products often have limited capacity despite generally being thicker, as they are fully reliant on the absorption capacity of the permeable fabric to deter leaks and ensure dryness. Newer designs such as a reusable period underwear includes a wicking fabric as the top layer coupled with an absorptive medium and a leakproof outer layer, however, they tend to be expensive.[10,11] Other reusable options such as menstrual cups can provide higher capacity and be worn for relatively longer periods of time. However, these are difficult to utilize in situations where privacy is lacking, and where lack of steady access to clean water renders safe reuse challenging.[2,3] In this article, we examine membranes with engineered wettability that permit unidirectional permeability of bodily fluids as low-cost and accessible alternatives.

[1]Department of Chemistry, Texas A&M University, College Station, TX 77842-3012, USA
[2]Department of Materials Science and Engineering, Texas A&M University, College Station, TX 77843-3003, USA
[3]Department of Chemistry, Texas A&M University at Qatar, Doha 23874, Qatar
[4]These authors contributed equally
[5]Lead contact
*Correspondence: rachelda@udel.edu (R.D.D.), banerjee@chem.tamu.edu (S.B.)
https://doi.org/10.1016/j.isci.2023.108224

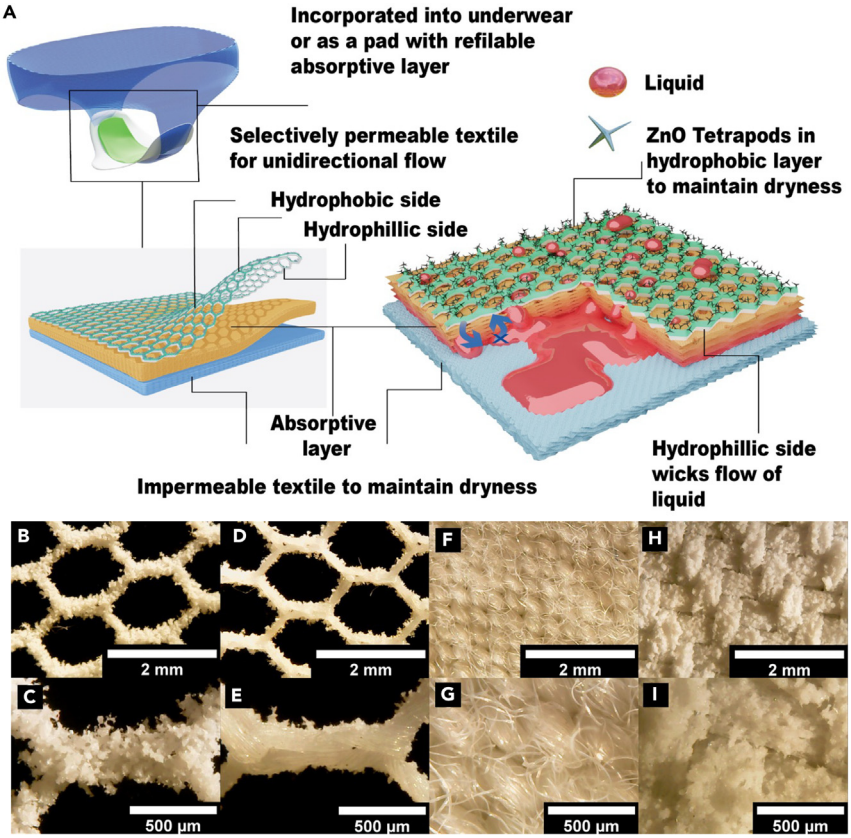

Figure 1. Schematic illustration of a fully assembled menstrual health solution

(A) Schematic depiction of an assembled menstrual hygiene system comprising a permeable porous Janus textile oriented such that the lyophobic side functionalized with ZnO-t textural elements faces the body, an absorptive middle layer, and a densely woven Janus fabric external layer, functionalized in the same way as the first layer, oriented such that the ZnO-t functionalized side faces the absorptive middle layer. Optical microscopy images of each of the layers of a ZnO-t/PDMS-based coated fabric at 2 mm and 500 µm.

(B and C) top, functionalized and (D and E) bottom, unfunctionalized sides of a Janus membrane prepared by coating 10.33 mg/cm^2 ZnO-t and PDMS onto one side of a porous polyester mesh mosquito netting; (F and G) an example absorptive middle-layer polyester fabric; and (H and I) a leakproof bottom layer formed by coating a densely woven polyester fabric with 10.33 mg/cm^2 ZnO-t with PDMS on one side. The coatings have been cast from 260 µL/cm^2 of 10 wt. % PDMS.

Surface modification and hierarchical texturation alter the permeability of textiles toward fluids.[12,13] "Janus" membranes, specifically, manifest asymmetric wettability on either membrane side and can be utilized to establish unidirectional mass transport such that a fluid irreversibly and spontaneously flows from the lyophobic to the lyophilic side of the membrane.[14,15] Liquid movement is guided by a balance of capillary forces. Movement across the lyophobic side is thermodynamically disfavored but is driven by the favorable interactions on the lyophilic side.[14,16,17] A delicate balance of surface energies across the two faces of the porous substrate is required to enable unidirectional permeation while alleviating backflow and enhance wicking. The pore dimensions, surface energies of the two opposite faces, and thickness of the layers allow for modulation of the driving forces for mass transport.[14] Careful tuning of these parameters has been key to establishing control over the unidirectional flow of biological fluids; some notable applications include wound-healing fabrics and moisture-wicking sportswear.[18–20] However, the application of this design idea in low-cost menstrual health solutions remains underexplored.

Interconnected ZnO tetrapodal (ZnO-t) networks have emerged as intriguing textural elements that can amplify the intrinsic (non)wettability of a surface by trapping a high density of plastronic air pockets.[21–27] Arrays of ZnO-t with protuberant arms imbue hierarchical texturation and can be coated onto textiles using a simple spray-on process to yield robust 3D hierarchically textured porosity, thereby alleviating the need for lithographic patterning to define surface roughness and reentrant curvature.[19–25,28,29] Integration of ZnO-t onto stainless steel mesh substrates followed by selective functionalization has enabled the effective separation of recalcitrant water/oil emulsions.[30–33] ZnO-t embedded onto stainless steel mesh manifests superhydrophobic and oleophilic character, which enables selective separation of wellhead emulsions with permeation of bitumen and retention of the aqueous phase.[26] Functionalization of the ZnO-t network with potassium perfluorooctanesulfonate switches the permeability, enabling permeation of the aqueous phase and retention of the oleic phase.[23]

Figure 1 sketches our design for the integration of ZnO-t onto textiles where the weave of the interlaced fabrics imbues micron-scale texturation to supplement the nanoscale topography derived from protuberant ZnO tetrapod arms. Such a configuration with multiscale

texturation provides a means to engender a wettability gradient, enabling unidirectional flow of menstrual fluids from the hydrophobic layer to the hydrophilic layer, but precluding flow in the reverse direction. In the configuration sketched in Figure 1, the layer facing the body is rendered hydrophobic, drawing the fluid through the pores of the fabric toward the hydrophilic side, thereby enabling rapid wicking. The fluid is drawn into the absorptive core along a gradient of increased wettability; back flow is prevented by the higher surface energy of the hydrophobic external surface, which gives rise to the capillary resistance as measured through wetback testing in subsequent sections. The positioning of the hydrophobic side toward the body further ensures dryness. Since components of hygiene products are in direct contact with the human body, they are subject to considerable regulatory oversight.[7,34,35] ZnO has been approved for use in a variety of products across food, packaging, and cosmetic industries. Moreover, as a semiconductor, ZnO-t, promotes the production of reactive oxygen species (ROS) under solar illumination, which imbues antibacterial function.[36] In this article, we describe the design, creation, and characterization of the Janus fabric and its integration within reusable pad or underwear designs through the addition of absorbent media and back-sheet layers (Figure 1). The assembled construct is readily washable, incorporates anti-microbial ZnO-t as the primary textural element, and is expected to offer greater comfort and discretion during wear as a result of the dryness afforded by both inner and outer layers. A series of standardized tests have been used to evaluate and benchmark the efficacy of the constructs.

RESULTS AND DISCUSSION

Design of Janus membranes with unidirectional fluid flow

Figure 1A schematically illustrates the design of the menstrual hygiene product, which comprises a reusable and washable pad or underwear with (i) a porous "Janus fabric" rendered selectively permeable to menstrual fluids by coating 100% polyester mesh mosquito netting with mixtures of polydimethylsiloxane (PDMS) and ZnO-t; (ii) a refillable absorptive layer, which can be adapted to any locally sourced absorbent; and (iii) an outer fabric that uses the same "Janus fabric" coating but is constructed from a densely woven or knitted fabric to generate an impermeable surface to maintain dryness and ensure discretion.

Figures 1B and 1C show optical microscopy images of the top, coated side of the ZnO-t/PDMS Janus membrane that faces the body and wicks menstrual fluid; Figures 1D and 1E show the uncoated side of the top Janus membrane; Figures 1F and 1G show optical images of an unfunctionalized absorptive middle layer, and Figures 1H and 1I show a densely woven fabric with similar ZnO-t/PDMS functionalization intended to serve as a leak-proof external layer.

Figures 2A–2D show scanning electron microscopy (SEM) images of the unfunctionalized side of the 100% polyester mosquito netting acquired at different magnifications. The images show interlaced strands that provide micron-scale texturation. Figures 2E–2H show corresponding SEM images of the opposite surface, which has been functionalized with 10.33 mg/cm^2 ZnO-t and PDMS. After curing, the resulting membrane shows hierarchical 3D texturation with protuberant arms of the ZnO tetrapods imbuing nanoscopic roughness. The ZnO tetrapods are embedded in the PDMS adhesion layer and the protuberant arms provide a randomly arrayed set of textural elements that strongly modify the interaction of liquid droplets with the surfaces (as displayed in the insets of Figures 2A and 2E). Water contact angles measured on the coated and uncoated sides of the mosquito netting are 155 $\pm$ 3° and 130 $\pm$ 6°, respectively (Table S1). Functionalization of one surface of the porous substrate thus establishes a gradient in wettability. This is the origin of driving force that enables liquids to permeate along a wettability gradient from the superhydrophobic to the hydrophobic side, affording a mechanism for wicking of menstrual fluids into the absorptive middle layer.

Figures S1 and S2 show analogous SEM and optical images, respectively, of the unfunctionalized polyester mosquito netting and mosquito netting coated with 260 μL/cm^2 10 wt. % PDMS on one side. Both present relatively smooth surfaces. The PDMS coating adheres to polyester and diminishes the inherent texturation provided by the weave of the fibers. The PDMS-functionalized polyester mesh shows a hydrophobic water contact angle of 142 $\pm$ 3°. Figure 3 shows the ATR-FTIR spectrum of the pristine polyester mosquito mesh netting substrate, the substrate functionalized with PDMS, and substrate functionalized with PDMS and ZnO-t. The characteristic IR bands of the polyester substrate at 1714 cm^{-1} arise from asymmetric and symmetric C=O stretching modes of the ester backbone. In addition, C–H stretching modes are observed at 2963 and 2905 cm^{-1}; aromatic C–H modes are observed at 1409 cm^{-1}. The bands at 1095 cm^{-1} and 1017 are characteristic of the C–O stretching modes of ester moieties, and finally the bands at 1340 cm^{-1} and 1242 cm^{-1} are from the C–O of the carbocyclic acid functional group.[37,38] Upon functionalization with PDMS, Si–C stretching modes are observed at 790 cm^{-1}; Si–O–Si stretching modes are observed at 1066 cm^{-1} and 1012 cm^{-1}; and C–H (from Si–CH_3) deformation modes are observed at 1258 cm^{-1}.[39–41] ZnO does not contribute any additional IR-active modes in the mid-IR region.

The SEM images in Figure 4 show the effects of varying the loading of ZnO-t on the texturation of the polyester meshes. Figure S3 shows corresponding optical microscopy images. Lower loadings of ZnO-t provide only a modest enhancement in texturation with the majority of embedded tetrapods being buried in the PDMS matrix (Figures 4A–4D and 4E–4H). Indeed, the coated substrates show water contact angles of 138 $\pm$ 7° and 139 $\pm$ 2°, respectively, which are essentially unmodified from the values measured for the PDMS coating alone (139 $\pm$ 5°). Hierarchical texturation is observed at higher loadings of ZnO-t, 10.33 mg/cm^2, as seen in Figures 2E–2H and Figures 1B, 1C; the water contact angle is increased to 155 $\pm$ 3°, manifesting a superhydrophobic surface. At a still higher loading of 20.67 mg/cm^2, the spray coating process and the curing of heavily ZnO-*t*-embedded PDMS becomes more challenging.

Functional performance of Janus membranes and fully assembled prototypes

To understand the effectiveness of the ZnO-t/PDMS-based Janus membranes in enabling unidirectional flow of menstrual fluids, a variety of potential absorbent fillers have been evaluated to enable testing of fully assembled prototypes (Figure 1A; Figures 5B, 5C), and to facilitate

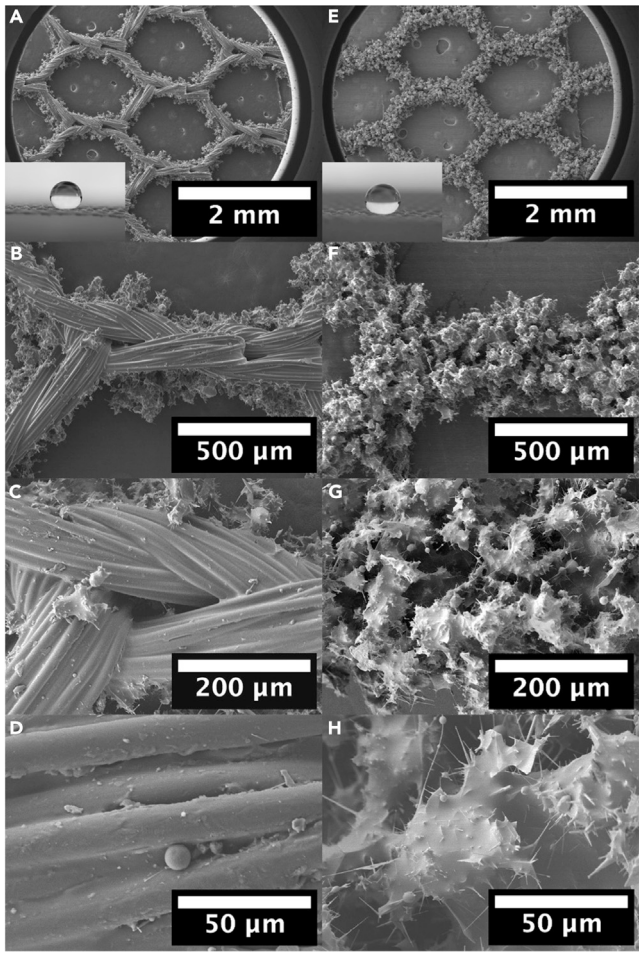

Figure 2. Texturization of dual-sided Janus membrane

(A–D) SEM images of the uncoated side of the Janus membrane.; the insets show water contact angles; (E–H) SEM images of 100% polyester mosquito netting coated with 10.33 mg/cm^2 ZnO-t and 260 µL/cm^2 of 10 wt.% PDMS. Scale bars, 2 mm, 500 µm, 200 µm, 50 µm. See also Table S1, and Figures S1, S2, S5, and S6.

comparison with commercially available products. The rate of longitudinal wicking and absorption as well as the absorption capacity of fabrics are affected not just by the inherent wettability of the fabric but also by the nature of the fabric construction. Attributes such as the fiber geometry, fiber density, yarn twisting level, and the weave pattern affect the nature of porosity across multiple length scales.[42–44] The test protocol for selection of the absorptive media is described in the STAR Methods section and different fabrics evaluated as absorption media are summarized in Table S2. Two layers of a double-brushed 90% polyester, 10% spandex fabric with a thickness of ca. 1.61 mm have been selected to serve as the absorbent fabric for testing of menstrual pad prototypes. This selection is based on the relatively high efficiency of absorption of this material, as well as its ability to effectively distribute the liquid through the thickness and breadth of the fabric after absorption, which provides a dryer feel.

The performance of ZnO-t/PDMS Janus membranes has been evaluated in fully assembled prototypes incorporating the absorbent filler material first by adapting standardized ISO 9073-13 and ISO 9073-14 methods. There are no current ISO standards that explicitly focus on the evaluation of menstrual hygiene products. ISO 9073-13 and ISO 9073-14 provide methods for evaluation of nonwoven cover stock fabrics for strike-through and wetback testing. These standards are designed primarily for quality control testing of the topmost, permeable layer of an absorptive product such as diapers. As such, these methods have been adapted here to enable testing of fully assembled products. Liquid strike-through testing evaluates the time required for the topmost permeable layer of an absorption product to allow for passage of saline solution through to the absorption layer. It thus serves as a probe of the efficacy with which the porous fabric is able to wick away menstrual fluids. Detailed testing protocols are described in the STAR Methods section and CAD drawings as well as photographs of the testing apparatus are provided in the Supporting Information. Briefly, during strike-through testing, three aliquots of a 1.20 mL aqueous saline solution are dispensed onto the menstrual care product at 1 min intervals. Subsequently, a simulated "baby weight" is placed on the menstrual pads for 3 min to allow the liquid to distribute throughout the absorptive layer and to simulate the pressure of typical activities such as sitting. The simulated "baby weight" is then removed, and an absorptive filter paper is placed between the simulated baby weight and the menstrual

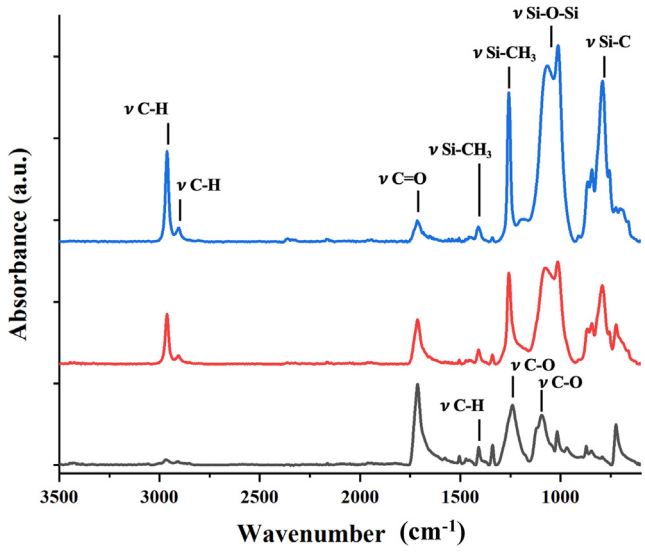

Figure 3. FTIR-ATR spectroscopy characterization

Infrared spectra of unfunctionalized polyester mesh (blue), polyester mesh coated with 260 μL/cm^2 of 10 wt.% PDMS (green), and polyester mesh coated with 260 μμL/cm^2 of 10 wt. % PDMS mixed with 10.33 mg/cm^2 ZnO-t.

pad for 2 min. The weight of liquid absorbed by the absorptive filter paper is recorded as the liquid wetback weight. The wetback test provides a measure of the ability of the functionalized fabrics to resist the transportation of the already permeated liquid back toward the body after absorption, and as such provides an indicator of dryness.

Results for testing of the ZnO-t/PDMS-based Janus membranes paired with two layers of absorptive fabric are presented in Table 1 and are benchmarked to several commercially available products. For comparison, testing has been additionally performed on an extensive set of control configurations, just two layers of the absorptive filler without a topmost permeable membrane, two layers of the absorptive filler with unfunctionalized polyester mesh as the topmost/body-facing layer, two layers of the absorptive filler with polyester mesh functionalized only with 15 mL 10% PDMS sans the ZnO-t textural elements, and two layers of the absorptive filler with polyester mesh functionalized with ZnO-t textural elements and PDMS. Different loadings of ZnO-t have further been evaluated with and without PDMS functionalization. Table 1 further includes a qualitative description of the state of the filter paper after wetback testing.

Average strike-through times of ZnO-t/PDMS-functionalized surfaces in fully assembled systems are modestly decreased from just the absorption media (13.87 $\pm$ 10.50 s) or unfunctionalized polyester meshes (Table 1). However, the strike-through times for ZnO-t/PDMS-based membranes are still longer, and have greater variation, than those measured for commercial pads. As an example, at a ZnO-t loading of 10.33 mg/cm^2, ZnO-t/PDMS-functionalized polyester meshes require 11.15 $\pm$ 12.90 s to strike-through to the absorptive middle layer as compared to 0.39–0.95 s for single-use products and 3.03–4.27 s for a reusable period product. This is primarily because although the absorptive filler demonstrates a relatively high absorption capacity and effectively distributes the liquid, its high strike-through time ultimately results in a higher value for the multilayer composite. Further, once the filler material is slightly wetted, the liquid strike-through times are greatly decreased. Indeed, the liquid strike-through times are substantially lower for the second and third aliquots of the saline solution, as shown in Figure S4B (see also Table S3). This is verified through a two-tailed, independent t-test between sequential strike-through times of our constructed pads (Table S4). The reported p values indicate that for all our pads fabricated with 2 layers of double-brushed polyester middle layer there is statistical significance between the initial strike-through time (when the fabric has not been wetted) and the strike-through time when the fabric has been previously wetted. This is illustrated by the p values all being < 0.05 when comparing the first/third, and the second/third strike-through times. Interestingly, when evaluating statistical difference between the second and third strike-through times, for all pads except those fabricated with 2.58 or 5.17 mg/cm^2 ZnO-t in the top-sheets, there was no significant difference. This suggests that once the pad is wetted, the strike-through time becomes more consistent, and is a better measure of the strike-through time likely to be observed throughout the day during use of the pad. The differences in strike-through times before and after wetting are likely a result of the metastable Cassie-Baxter wetting regimes—which initially pin liquid droplets at surface asperities.

Inclusion of a thin (ca. $<$ 1 mm) 100% polyester liner layer that has superhydrophilic character (but minimal absorptive capacity) between the functionalized Janus membrane and absorptive layers reduces the strike-through time for the ZnO-t/PDMS-functionalized polyester mesh membrane to 7.81 $\pm$ 4.62 s. This suggests the strike-through time is a function of the absorptive medium rather than the Janus membranes. The dependency of the strike-through time on the composition of the middle layer has been further analyzed with the three other middle layers, fleece, 100% cotton, and 100% knitted polyester fabrics. When tested with the optimized 10.33 mg/cm^2 Janus membrane top-sheet, the resulting average strike-through times are 0.93 $\pm$ 0.63, 8.46 $\pm$ 7.67, and 4.03 $\pm$ 2.51 s, respectively, for fleece, 100% cotton, and 100% knitted polyester (Table S2), corroborating the primary dependence of the strike-through time on the absorptive media. Figure S4B plots the

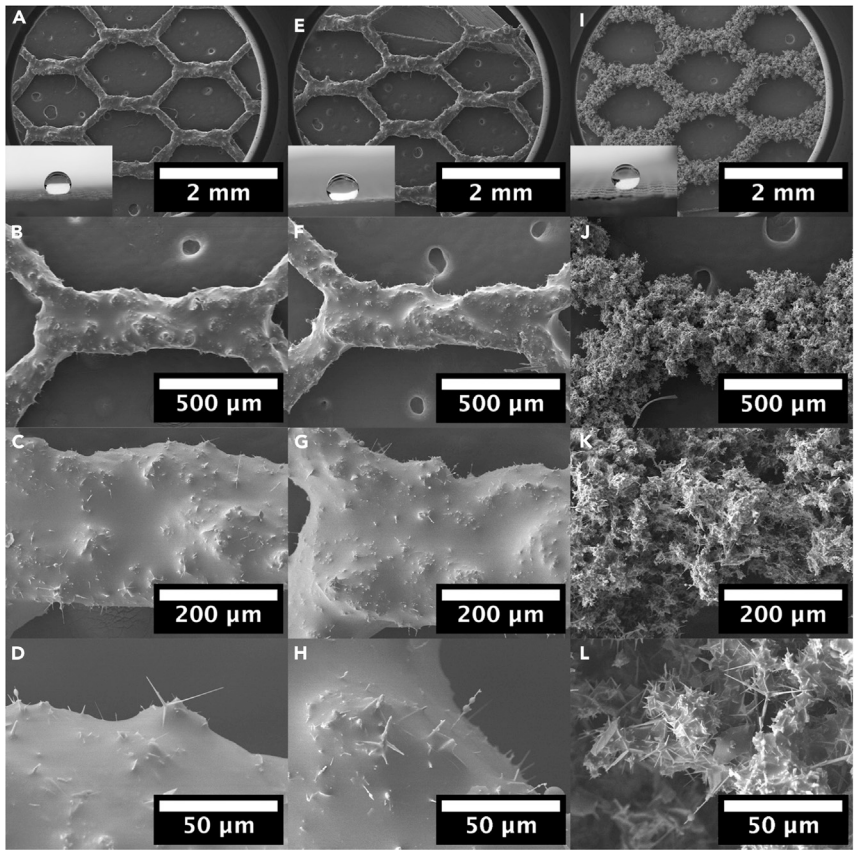

Figure 4. Effect of ZnO Loading on texturation

SEM images, in increasing magnification, of polyester meshes with different loadings of ZnO-t (A–D) 2.58; (E–H) 5.17; and (I–L) 20.67 mg/cm^2 ZnO-t. The PDMS amount is held constant at 260 µL/cm^2. Water contact angle images of the functionalized mosquito nettings with respectively ZnO-t and PDMS loadings are shown as insets of A, E, and I. Scale bars, 2 mm, 500 µm, 200 µm, 50 µm. See also Figure S3.

strike-through time as a function of the ZnO-t loading in ZnO-t/PDMS-functionalized polyester meshes. The p values resulting from t tests performed on the strike-through times further emphasize the dominant effect that the middle-layer composition has on the strike-through time. Indeed, the trend observed in decreasing strike-through times and its difference is not as strong with the different middle cores (Table S4). The Janus membrane does, however, improve the strike-through time in comparison to the absorptive layer alone. Notably, for these alternative absorptive layers, different from the down-selected absorptive medium, the strike-through time increases for the third aliquot. This is a result of the middle layer reaching full saturation at lower volumes resulting in decreased efficacy of wicking. The results demonstrate the need to strike a balance between a reasonable strike-through time and efficacy of wicking, absorptive capacity, and overall product thickness.

We next turn our attention to the wetback testing results in Table 1. The absorptive filler material alone and the absorptive filler coupled with a top layer of unfunctionalized polyester mesh provide minimal protection against liquid wetback with measured values of 929 $\pm$ 122 and 853 $\pm$ 104 mg, respectively, for the saline test liquid. It is worth noting that measurements above 500 mg correspond to near complete wetting of the absorptive filter paper (noted in Table 1). Upon coating the polyester mesh with 260 µL/cm^2 10 wt. % PDMS on one side, substantial improvements were observed in the liquid wetback, which is decreased down to 53 $\pm$ 38 mg. Embedding ZnO-t in the PDMS matrix initially increases the mass of liquid wetback; however, with an increase in the ZnO-t loading from 2.58 to 5.11 and then to 10.33 mg/cm^2, the wetback mass decreases from 79 $\pm$ 78 mg to 35 $\pm$ 20 mg and to 27 $\pm$ 7 mg, respectively (Figure S4A). These results are attributable to the exceptional capillary resistance resulting from the coating, which enforces unidirectional flow. Notably, the lowest values of wetback recorded are consistently around 20–30 mg, which correspond to minimal or entirely absent visual indications of a leak. In contrast, wetback masses close to 40 mg or higher are inevitably accompanied by the appearance of array of spots. No visual observations of liquid wetback have been observed across multiple replicates for the 10.33 mg/cm^2 ZnO-t/PDMS-functionalized polyester mesh coupled with the two layers of absorptive material. This assembled system provided far superior protection against liquid wetback as compared to commercially available reusable products while maintaining a comparable total prototype thickness (Table 1). The reusable fleece-based pad demonstrated an average of 51 $\pm$ 55 mg liquid wetback with frequent appearance of visual breakthrough spots, whereas the reusable period underwear demonstrated an average of 686 $\pm$ 123 mg liquid wetback, representing near complete saturation of the filter paper. The 10.33 mg/cm^2 ZnO-t/PDMS-functionalized

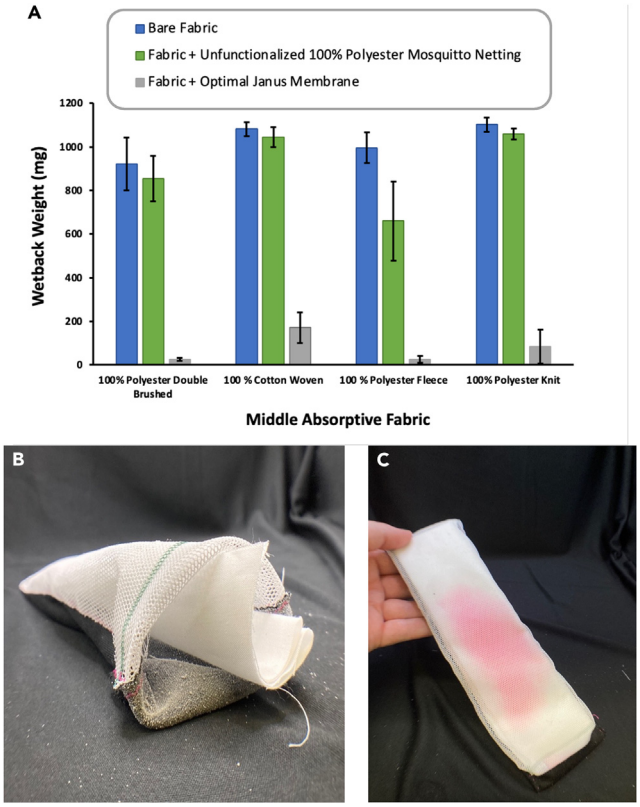

Figure 5. Wetback weights of assembled products with various absorptive fabrics and fully assembled prototypes

(A) Wetback weight of the bare middle absorptive layer (blue), middle absorptive layer with an unfunctionalized 100% polyester mosquito netting top-sheet (green), and middle absorptive layer with a 10.33 mg/cm^2 ZnO-t Janus membrane top sheet (gray).

(B) A fully assembled prototype showing the three distinct layers: black coated impermeable back-sheet, cotton middle, removable, absorptive layer, and porous Janus membrane with 10.33 mg/cm^2 ZnO-t and 260 μL/cm^2 of 10 wt. % PDMS.

(C) Aerial view of assembled prototype. See also Tables S3–S5.

polyester mesh coupled with the two layers of absorptive material indeed demonstrates performance comparable to single-use pads embedded with engineered polymers and superior to those that have cotton or cellulose as absorbent media (Table 1) Further increasing the loading of ZnO-t did not further enhance performance; a fully assembled system with 20.67 mg/cm^2 ZnO-t loading in PDMS demonstrates a wetback mass of 35 $\pm$ 13 mg and shows the emergence of small breakthrough spots that increase in size upon extended testing. The higher loading of ZnO-t further enhances the hierarchical texturation (Figures 2 and 3). The rougher surfaces can indeed trap saline droplets in metastable configurations, which disrupts wettability gradients. A similar degradation of anti-icing behavior was observed for ZnO-t embedded onto stainless steel meshes with increasing loading as a result of the trapping of water droplets by rough surfaces.[45]

The Janus membrane with a ZnO-t loading of 10.33 mg/cm^2 has further been tested as a top-sheet using wet back and strike-through testing with various other absorptive middle layers to ensure a broad range of use. The absorptive middle layers have been chosen to keep a similar overall product thickness and maintain an acceptable absorption capacity. Specifically, 100% polyester fleece, 100% cotton, and 100% polyester knit fabrics have been evaluated. As shown in Figure 5, upon the addition of the Janus membrane, the wetback weights are decreased on average by 1.5 orders of magnitude as compared to both the fabric alone and the fabric with unfunctionalized polyester mesh as a top sheet. The fleece absorptive middle layer shows the lowest wetback weight of 26 $\pm$ 17 mg with no visual indications of leaks. This performance is comparable to a commercially available pad based on a superabsorbent polymer and outcompetes all other commercial single-use and reusable materials examined in this work. The tabulated wetback weights and visual observations are summarized in Table S5. The wetback weight can be further reduced through incorporation of additional fabric layers or by inclusion of absorptive media with a higher absorption capacity. The double-brushed knit (90% polyester, 10% spandex) fabric has been down-selected as the middle-layer absorption media from choices evaluated in Table S2.

Embedding ZnO-t within the PDMS adhesion layer on polyester mesh furthermore improves the softness of the fabric. Higher ZnO-t loadings reduce the friction of the fabric and increase the softness to touch. Without ZnO-t, the PDMS coated mosquito netting presents a rubbery feel, consistent with the high coefficient of friction of PDMS (ca. 1).[46] The noticeable enhancement in softness upon addition of ZnO-t is likely due to the change in surface texture, which reduces the effective contact area with other surfaces.[47] Inclusion of relatively hard materials such

Table 1. Liquid wetback and strike-through times of the Janus membranes benchmarked to commercial single-use and reusable pads

Menstrual care product top sheet description	Strike-through Time average (s)	Wetback (mg)	Visual indications of leaks	Product total thickness (mm)
2 Layers 100% Polyester Double-Brushed Absorptive Middle Fabrics				
None	13.87 ± 10.50	929 ± 122	Saturation Consistently Observed	1.61
Unfunctionalized Polyester Mesh	14.97 ± 13.07	853 ± 104	Saturation Consistently Observed	1.64
Polyester Mesh functionalized with 260 μL/cm^2 10 wt. % PDMS	2.83 ± 2.23	53 ± 38	Spots Observed	1.67
Polyester Mesh functionalized with 260 μL/cm^2 10 wt. % PDMS +2.58 mg/cm^2 ZnO-t	21.26 ± 25.98	79 ± 78	Spots Observed	1.67
Polyester Mesh functionalized with 260 μL/cm^2 10 wt. % PDMS +5.17 mg/cm^2 ZnO-t	19.98 ± 23.16	35 ± 20	Few Spots Observed	1.76
Polyester Mesh functionalized with 260 μL/cm^2 10 wt. % PDMS +10.33 mg/cm^2 ZnO-t	11.15 ± 12.90	27 ± 7	No Spots Observed	1.81
Polyester Mesh functionalized with 260 μL/cm^2 10 wt. % PDMS +20.67 mg/cm^2 ZnO-t	27.64 ± 35.09	35 ± 13	Few Spots Observed	2.02
2 Layers 100% Polyester Double-Brushed +1 layer 100% Polyester Liner Absorptive Middle Fabrics				
Polyester Mesh functionalized with 260 μL/cm^2 10 wt. % PDMS +10.33 mg/cm^2 ZnO-t	7.81 ± 4.62	37 ± 6	No Spots Observed	1.91
Polyester Mesh functionalized with 260 μL/cm^2 10 wt. % PDMS	12.03 ± 16.86	41 ± 56	Few Spots Observed	1.68
Single Use Pad 1- Super Absorbent Polymer Absorptive Middle Material				
Polypropylene Nonwoven Cover Stock	0.49 ± 0.22	25 ± 4	No Spots Observed	2.86
Single Use Pad 2- Super Absorbent Polymer Absorptive Middle Material				
Cotton Nonwoven Cover Stock	0.61 ± 0.33	41 ± 19	Spots Observed	3.40
Single Use Pad 3 – Cellulose and Super Absorbent Polymer Absorptive Middle Material				
Cotton Nonwoven Cover Stock	0.39 ± 0.17	134 ± 31	Spots Observed	3.19
Single Use Pad 4- Cellulose, Cotton, and Super Absorbent Polymer Absorptive Middle Material				
Cotton Nonwoven Cover Stock	0.95 ± 0.29	632 ± 62	Saturation Consistently Observed	3.06
Reusable Period Underwear – Unspecified Absorbent Core				
Unspecified Fabric Layer	3.69 ± 1.97	646 ± 139	Saturation Consistently Observed	1.85
Reusable Pad – Bamboo Charcoal Fiber				
None	3.03 ± 4.17	51 ± 55	Few Spots Observed	2.09

The reported total thickness for non-commercial products does not include the impermeable lower layer. n = 5 See also Tables S3 and S4 and Figure S4.

as glass beads, or in this case ZnO-t, to the soft PDMS matrix has also been shown to increase the matrix stiffness and reduce compression depth during friction testing. A decrease in compression depth decreases the contact area between the testing tip and the sample surface, which enables better distribution of stress, resulting in a reduction of the coefficient of friction.[48]

The durability of the ZnO-t/PDMS Janus membranes toward washing has been evaluated by subjecting a membrane formed by coating 10.33 mg/cm^2 ZnO-t with260 μL/cm^2 10 wt. % PDMS through a standard washing machine and by separately hand washing five times as described in the STAR Methods section. SEM images shown in Figure S5, and optical microscopy images shown in Figure S6 show that the ZnO tetrapods remain intact and that hierarchical texturation is preserved upon washing. Further, the contact angles remain unaffected by the washing processes with the machine-washed sample showing an average contact angle of 152 ± 3° and the hand-washed sample showing an average contact angle of 156 ± 1° after machine washing (compared to an original value of 155 ± 3°) illustrating that the coating retains its superhydrophobic character.

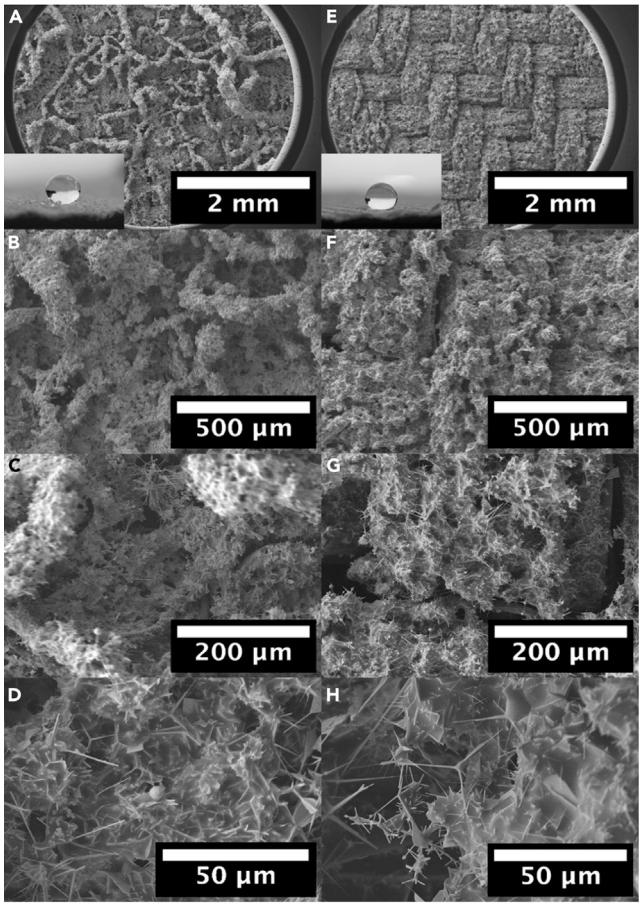

Figure 6. Microstructure of external layer

SEM images of leakproof lower layers formed by coating densely woven (A–D) 100% cotton and (E–H) 100% polyester fabrics both coated with 10.33 mg/cm^2 ZnO-t and 260 µL/cm^2 10 wt. % PDMS on one side. Scale bars, 2 mm, 500 µm, 200 µm, 50 µm. See also Figure S7.

Design of reusable leak-proof backing

Fully assembled menstrual care products additionally require a leakproof external layer to ensure that liquid captured by the absorptive fabric is contained. Two leakproof external fabric layers have been designed utilizing the same coating formulation and process as the porous Janus membranes. Figure 6 shows SEM images of densely woven 100% cotton and polyester fabrics coated on one side with 10.33 mg/cm^2 ZnO-t and 260 µL/cm^2 10 wt. % PDMS. Corresponding optical microscopy images are shown in Figure S7. The coating renders the originally superhydrophilic polyester fabric, which has a contact angle of 0°, superhydrophobic, with a contact angle of 151 $\pm$ 4°. Similarly, the 100% cotton fabric is transformed from being unevenly hydrophobic to a stable superhydrophobic surface with a contact angle of 155 $\pm$ 1°. The superhydrophobic behavior of the coated polyester and cotton fabrics are fully compatible with any combination of top layer and absorption medium. These coatings have been similarly tested using adapted ISO 9073-13 and ISO 9073-14 methods.

Liquid strike-through testing has been performed on two layers of the chosen absorptive filler material, which results in the fabric being saturated with a total of 3.60 mL saline solution. The functionalized densely woven, clothing facing fabrics are then placed with the functionalized side facing the wetted absorbent layer. A simulated baby weight is then placed on top for 3 min. The simulated baby weight is subsequently removed in order to allow for placement of the absorbent filter paper between the upward-facing unfunctionalized fabric and the simulated baby weight. Liquid wetback masses are then recorded based on the mass of liquid absorbed by the filter paper (Table 2). The results show very low wetback weights of 15 $\pm$ 3 and 26 $\pm$ 25 mg for a densely woven polyester and cotton fabric, respectively, which is indicative of the efficacy of the coating in yielding back sheets that maintain discretion and prevent leaks on different fabric compositions.

Simulated menstrual fluid testing

We next turn our attention to a more realistic test fluid. Menstrual fluid is a complex and inhomogeneous mixture of endometrial tissue, blood, and cervico-vaginal secretions. Its composition and resulting physical properties vary across individuals and throughout the menstrual cycle.[49,50] The proportion of menstrual fluid that is blood varies greatly, with reports ranging from 1.6–81.7 vol. %.[51] Compared to venous blood,

Table 2. Liquid wetback and contact angle of the lower impermeable layers

Cloth-facing samples	Liquid wetback (mg)	Visual indication of leaks
Densely Woven 100% Polyester	749 ± 79	Saturation Consistently Observed
Densely Woven Polyester +10.33 mg/cm^2 ZnO-t + PDMS	15 ± 3	No Spots Observed
Densely Woven 100% Cotton	797 ± 80	Saturation Consistently Observed
Densely Woven 100% Cotton +10.33 mg/cm^2 ZnO-t + PDMS	26 ± 25	No Spots Observed

n = 15.

menstrual fluid has a higher water content and does not exhibit coagulation,[52] although agglomerates of tissue and tissue are observed. Viscosity of menstrual fluid varies greatly ranging from a few centipoises to several hundred centipoises, and this fluid is often significantly more viscous than venous blood.[53] Cervical mucus imbues a high and variable elasticity, and the surface tension of menstrual fluid is lower than water at around 50 mN/m.[50] Given the complexity of menstrual fluids we recognize the limitations of saline media as a test fluid. Blood simulants are similarly limited in their ability to emulate the rheological and adhesion characteristics of menstrual fluids. As such, we have examined the function of our prototypes used a simulated menstrual fluid as a more realistic test fluid. This fluid has a pH of ca. 7.4, a viscosity of ca. 10 cp, a measured surface tension of 51.54 ± 0.27 mN/m, and a composition emulative of menstrual fluids aside for tissue agglomerations.

Testing was performed for the fully assembled prototype using the same exact conditions and methods used for the saline solution. Table 3 lists strike-through times measured with the simulated menses fluid. The measured value of 13.34 ± 7.37 s is comparable to the initial strike-through time of 13.87 ± 10.50 s measured for saline media. However, as listed in Table S6, the trend of the three sequential strike-through times observed with saline media is reversed, and the strike-through time is gradually increased across the 3 aliquots. This observation suggests the absorptive core medium more rapidly approaches saturation. Table S6 shows that the strike-through times become rather become consistent across the three aliquots of menses fluids after inclusion of a top-sheet. With the inclusion of an unfunctionalized polyester mesh top-sheet, the average strike-through time decrease to 4.89 ± 1.38 s suggesting that the inclusion of the textured mesh under the pressure of the strike-through plate creates a better wetting environment for the menstrual fluid simulant. Upon the full functionalization of the polyester mesh with 260 μL/cm^2 10 wt. % PDMS mixed with 10.33 mg/cm^2 ZnO-t, the strike-through time increases to 8.85 ± 2.80 s. This is likely again due to metastable pinning of the simulated menstrual fluid as observed in the saline solution tests.

In wetback testing, the weight with the inclusion of the polyester mesh with 260 μL/cm^2 10 wt. % PDMS mixed with 10.33 mg/cm^2 ZnO-t top-sheet was 217 ± 87 mg, which is greater than the 27 ± 7 mg wetback weight of the same pad tested with saline media. The increase in wetback weight is a result of the lower surface tension of the simulated menstrual fluids, which decreases the capillary resistance. However, inclusion of the Janus membrane still shows improved efficacy. It is notable that while menstrual fluid simulant is a more realistic test liquid as compared to saline media, further testing is required under clinically relevant conditions.

Conclusions

A textile-based Janus membrane has been designed by embedding ZnO-t in a PDMS matrix coated onto one side of a porous polyester mesh mosquito net, which renders the surface superhydrophobic and thereby establishes a wettability gradient between the two sides of the membrane. Unidirectional wicking of saline solution is observed when the uncoated, hydrophobic side of the polyester mosquito netting is interfaced with a superhydrophilic polyester liner coupled with two layers polyester absorbent media. The assembled prototype resists flow in the opposite direction even upon addition of over 1 kg of applied weight. A ZnO-t loading of 10.33 mg/cm^2 has been found to be optimal to achieve hierarchical texturation, and homogeneous surface coverage, thereby enabling rapid unidirectional flow. At this loading of ZnO-t,

Table 3. Liquid wetback and strike-through times of the Janus membranes with the simulated menstrual fluid as the probe liquid

Menstrual care product top sheet description	Strike-through Time average (s)	Wetback (mg)	Visual indications of leaks	Product total thickness (mm)
2 Layers 100% Polyester Double-Brushed Absorptive Middle Fabrics				
None	13.34 ± 7.37	833 ± 61	Saturation Consistently Observed	1.61
Unfunctionalized Polyester Mesh	4.89 ± 1.38	687 ± 63	Saturation Observed Where Pressure Applied	1.64
Polyester Mesh functionalized with 260 μL/cm^2 10 wt. % PDMS	6.21 ± 1.98	153 ± 121	Spots Observed	1.67
Polyester Mesh functionalized with 260 μL/cm^2 10 wt. % PDMS +10.33 mg/cm^2 ZnO-t	8.85 ± 2.80	217 ± 87	Spots Observed	1.81

The reported total thickness for non-commercial products does not include the impermeable lower layer. n = 5 See also Table S6.

the coated surface exhibits a water contact angle of 155° ± 3°. A fully assembled prototype has been designed that combines the ZnO-t/PDMS-coated polyester mesh Janus membranes and absorptive filler layers with a leak-proof backing layer designed by similarly coating densely woven cotton or polyester fabrics with ZnO-t/PDMS. The coated substrates show preservation of differential wettability, wicking efficacy, and absorptive capacity after hand- or machine washing. In addition to saline, a simulated menstrual fluid is used in the performance testing of constructed pads. The results show promise and efficacy in creating unidirectional flow and leak prevention but demonstrate the need for greater capillary resistance with more biologically realistic lower surface tension fluids. The results indicate the promise of robust Janus textiles in the design of innovative, inexpensive, and accessible hygiene products that allow for the rapid unidirectional wicking of menstrual fluids, high absorption capacity, dryness, and discretion. The coating approach is generalizable to locally sourced textiles, and thus represents a promising practical solution to address the menstrual health needs of menstruating individuals in lower- and middle-income communities.

Limitations of the study

One of the main limitations of this study is performance of the fabricated menstrual pads under in-use conditions. Variations of menstrual fluid rheology during cycles and between menstruators, will likely modify performance results. Further modification of the Janus membrane and impermeable back sheet may be necessary for optimal performance under application.

STAR★METHODS

Detailed methods are provided in the online version of this paper and include the following:

- KEY RESOURCES TABLE
- RESOURCE AVAILABILITY
  - Lead contact
  - Materials availability
  - Data and code availability
- METHOD DETAILS
  - Materials
  - ZnO synthesis
  - Fabric functionalization
  - Coating characterization
  - Performance and durability evaluation: middle layer absorption capacity
  - Performance and durability evaluation: repeated liquid strike-through time
  - Performance and durability evaluation: wetback test
  - Performance and durability evaluation: menstrual fluid simulant
  - Performance and durability evaluation: washability
  - Surface tension testing of simulated menstrual fluids

SUPPLEMENTAL INFORMATION

Supplemental information can be found online at https://doi.org/10.1016/j.isci.2023.108224.

ACKNOWLEDGMENTS

The authors gratefully acknowledge partial support from the National Science Foundation under IIP 2122604. L.D.D. was partially supported by a Hagler Institute of Advanced Studies HEEP fellowship. The research of K.S. was supported by the National Science Foundation under CHE 1851936. R.D.D. acknowledges support from the Intelligence Community Postdoctoral Research Fellowship Program administered by Oak Ridge Institute for Science and Education (ORISE) through an interagency agreement between the U.S. Department of Energy and the Office of the Director of National Intelligence (ODNI). TES acknowledges the support of National Science Foundation under a Graduate Research Fellowship grant DGE: 1746932. Use of the TAMU Materials Characterization Facility and Soft Matter Facility is acknowledged.

AUTHOR CONTRIBUTIONS

Conceptualization, S.L.S., L.D.D., and R.D.D.; Methodology, S.L.S., L.D.D., and R.D.D.; Investigation, S.L.S., L.D.D., T.E.S., K.S., N.P., E.W., and R.D.D.; Data Curation, S.L.S.; Writing - Original Draft, S.L.S., L.D.D., and R.D.R.; Formal Analysis, S.L.S., L.D.D., and R.D.R.; Project administration S.B. and R.D.D.; Writing - Review & Editing, S.L.S., L.D.D., T.E.S., K.S., N.P., C.L., E.W., M.A., L.F., R.D.D., and S.B.; Validation, S.B. and R.D.D; Supervision, R.D.D. and S.B.; Funding Acquisition, S.B.

DECLARATION OF INTERESTS

A provisional patent has been filed related to this work.

INCLUSION AND DIVERSITY

One or more of the authors of this paper self-identifies as an underrepresented ethnic minority in their field of research or within their geographical location. One or more of the authors of this paper self-identifies as a gender minority in their field of research. One or more of the authors of this paper self-identifies as a member of the LGBTQIA+ community.

Received: June 27, 2023
Revised: September 15, 2023
Accepted: October 12, 2023
Published: November 3, 2023

REFERENCES

1. Kuhlmann, A.S., Henry, K., and Wall, L.L. (2017). Menstrual Hygiene Management in Resource-Poor Countries. Obstet. Gynecol. Surv. *72*, 356–376. https://doi.org/10.1097/OGX.0000000000000443.
2. Sumpter, C., and Torondel, B. (2013). A Systematic Review of the Health and Social Effects of Menstrual Hygiene Management. PLoS One *8*, e62004. https://doi.org/10.1371/journal.pone.0062004.
3. Sommer, M., Caruso, B.A., Sahin, M., Calderon, T., Cavill, S., Mahon, T., and Phillips-Howard, P.A. (2016). A Time for Global Action: Addressing Girls' Menstrual Hygiene Management Needs in Schools. PLoS Med. *13*, e1001962. https://doi.org/10.1371/journal.pmed.1001962.
4. House, S., Mahon, T., and Cavill, S. (2013). Menstrual Hygiene Matters: A Resource for Improving Menstrual Hygiene around the World. Reprod. Health Matters *21*, 257–259. https://doi.org/10.1016/s0968-8080(13)41712-3.
5. Sebert Kuhlmann, A., Peters Bergquist, E., Danjoint, D., and Wall, L.L. (2019). Unmet Menstrual Hygiene Needs among Low-Income Women. Obstet. Gynecol. *133*, 238–244. https://doi.org/10.1097/AOG.0000000000003060.
6. Ajmeri, J.R., and Ajmeri, C.J. (2016). Developments in the Use of Nonwovens for Disposable Hygiene Products. Advances in Technical Nonwovens, 473–496. https://doi.org/10.1016/B978-0-08-100575-0.00018-8.
7. Woeller, K.E., and Hochwalt, A.E. (2015). Safety Assessment of Sanitary Pads with a Polymeric Foam Absorbent Core. Regul. Toxicol. Pharmacol. *73*, 419–424. https://doi.org/10.1016/J.YRTPH.2015.07.028.
8. Zohuriaan-Mehr, M.J., and Kabiri, K. (2008). Superabsorbent Polymer Materials: A Review. Polymer Journal. Iranian Polymer Journal *17*, 451.
9. Choudhary, H., Zhou, C., and Raghavan, S.R. (2023). A Better Picker-Upper: Superabsorbent "Gel Sheets" with Fabric-like Flexibility. Matter *6*, 521–536. https://doi.org/10.1016/j.matt.2022.11.021.
10. Dunbar, A., Agrawal, A., and Agrawal, R. (2017). Moisture Wicking and Leak Resistant Underwear Garments. EP 2 879 534 B1. https://register.epo.org/application?number=EP13825422.
11. Griffiths, J. (2014). Absorbent Garment. WO 176677 A1. Griffiths, J. Absorbent Garment, US10441480B2, US Patent 10,441,480. https://patentcenter.uspto.gov/applications/15833248.
12. Kota, A.K., Kwon, G., and Tuteja, A. (2014). The Design and Applications of Superomniphobic Surfaces. NPG Asia Mater. *6*, 109. https://doi.org/10.1038/am.2014.34.
13. Zahid, M., Mazzon, G., Athanassiou, A., and Bayer, I.S. (2019). Environmentally Benign Non-Wettable Textile Treatments: A Review of Recent State-of-the-Art. Adv. Colloid Interface Sci. *270*, 216–250. https://doi.org/10.1016/j.cis.2019.06.001.
14. Li, H.-N., Yang, J., Xu, Z.-K., Li, H.-N., Yang, J., and Xu, Z.-K. (2020). Asymmetric Surface Engineering for Janus Membranes. Adv. Mater. Interfaces *7*, 1902064. https://doi.org/10.1002/ADMI.201902064.
15. Yang, H.C., Hou, J., Chen, V., and Xu, Z.K. (2016). Janus Membranes: Exploring Duality for Advanced Separation. Angew. Chem. Int. Ed. Engl. *55*, 13398–13407. https://doi.org/10.1002/ANIE.201601589.
16. Tian, X., Li, J., and Wang, X. (2012). Anisotropic Liquid Penetration Arising from a Cross-Sectional Wettability Gradient. Soft Matter *8*, 2633–2637. https://doi.org/10.1039/C2SM07111H.
17. Yang, J., Li, H.-N., Chen, Z.-X., He, A., Zhong, Q.-Z., and Xu, Z.-K. (2019). Janus Membranes with Controllable Asymmetric Configurations for Highly Efficient Separation of Oil-in-Water Emulsions. J. Mater. Chem. A Mater. *7*, 7907–7917. https://doi.org/10.1039/C9TA00575G.
18. Wang, X., Huang, Z., Miao, D., Zhao, J., Yu, J., and Ding, B. (2019). Biomimetic Fibrous Murray Membranes with Ultrafast Water Transport and Evaporation for Smart Moisture-Wicking Fabrics. ACS Nano *13*, 1060–1070. https://doi.org/10.1021/acsnano.8b08242.
19. Dong, Y., Kong, J., Phua, S.L., Zhao, C., Thomas, N.L., and Lu, X. (2014). Tailoring Surface Hydrophilicity of Porous Electrospun Nanofibers to Enhance Capillary and Push-Pull Effects for Moisture Wicking. ACS Appl. Mater. Interfaces *6*, 14087–14095. https://doi.org/10.1021/am503417w.
20. Zhou, H., Wang, H., Niu, H., Zeng, C., Zhao, Y., Xu, Z., Fu, S., Lin, T., Zhou, H., Wang, H., et al. (2016). One-Way Water-Transport Cotton Fabrics with Enhanced Cooling Effect. Adv. Mater. Interfaces *3*, 1600283. https://doi.org/10.1002/ADMI.201600283.
21. Mishra, Y.K., and Adelung, R. (2018). ZnO Tetrapod Materials for Functional Applications. Mater. Today *21*, 631–651. https://doi.org/10.1016/j.mattod.2017.11.003.
22. Mishra, Y.K., Modi, G., Cretu, V., Postica, V., Lupan, O., Reimer, T., Paulowicz, I., Hrkac, V., Benecke, W., Kienle, L., and Adelung, R. (2015). Direct Growth of Freestanding ZnO Tetrapod Networks for Multifunctional Applications in Photocatalysis, UV Photodetection, and Gas Sensing. ACS Appl. Mater. Interfaces *7*, 14303–14316. https://doi.org/10.1021/acsami.5b02816.
23. Bajpayee, A., Alivio, T.E.G., McKay, P., and Banerjee, S. (2019). Functionalized Tetrapodal ZnO Membranes Exhibiting Superoleophobic and Superhydrophilic Character for Water/Oil Separation Based on Differential Wettability. Energy Fuels *33*, 5024–5034. https://doi.org/10.1021/acs.energyfuels.9b00718.
24. Davidson, R.D., O'Loughlin, T.E., Alivio, T.E.G., Lim, S.M., and Banerjee, S. (2022). Thermodynamics of Wettability: A Physical Chemistry Laboratory Experiment. J. Chem. Educ. *99*, 2689–2696. https://doi.org/10.1021/acs.jchemed.2c00243.
25. O'Loughlin, T.E., Martens, S., Ren, S.R., McKay, P., and Banerjee, S. (2017). Orthogonal Wettability of Hierarchically Textured Metal Meshes as a Means of Separating Water/Oil Emulsions. Adv. Eng. Mater. *19*, 1600808. https://doi.org/10.1088/1748-3190/aaa1c1.
26. O'Loughlin, T.E., Ngamassi, F.-E., McKay, P., and Banerjee, S. (2018). Separation of Viscous Oil Emulsions Using Three-Dimensional Nanotetrapodal ZnO Membranes. Energy Fuels *32*, 4894–4902. https://doi.org/10.1021/acs.energyfuels.8b00235.
27. O'Loughlin, T.E., Dennis, R.V., Fleer, N.A., Alivio, T.E.G., Ruus, S., Wood, J., Gupta, S., and Banerjee, S. (2017). Biomimetic Plastronic Surfaces for Handling of Viscous Oil. Energy Fuels *31*, 9337–9344. https://doi.org/10.1021/acs.energyfuels.7b01877.
28. Athauda, T.J., Hari, P., and Ozer, R.R. (2013). Tuning Physical and Optical Properties of ZnO Nanowire Arrays Grown on Cotton Fibers. ACS Appl. Mater. Interfaces *5*, 6237–6246. https://doi.org/10.1021/am401229a.
29. Wang, Y.W., Shen, R., Wang, Q., and Vasquez, Y. (2018). ZnO Microstructures as Flame-Retardant Coatings on Cotton Fabrics. ACS Omega *3*, 6330–6338. https://doi.org/10.1021/acsomega.8b00371.
30. Douglas, L.D., Rivera-Gonzalez, N., Cool, N., Bajpayee, A., Udayakantha, M., Liu, G.-W., Anita, Banerjee, S., and Banerjee, S. (2022). A Materials Science Perspective of Midstream Challenges in the Utilization of Heavy Crude Oil. ACS Omega *7*, 1547–1574. https://doi.org/10.1021/acsomega.1c06399.
31. O'Loughlin, T.E., Waetzig, G.R., Davidson, R.E., Dennis, R.V., and Banerjee, S. (2017). Modifying Base Metal Substrates to Exhibit Universal Non-Wettability: Emulating Biology and Going Further. In Encyclopedia of Inorganic and Bioinorganic Chemistry, R.A. Scott, ed., pp. 1–21. https://doi.org/10.1002/9781119951438.eibc2493.
32. Söz, Ç.K., Trosien, S., and Biesalski, M. (2020). Janus Interface Materials: A Critical Review and Comparative Study. ACS Mater. Lett. *2*,

336–357. https://doi.org/10.1021/acsmaterialslett.9b00489.

33. Zhou, H., and Guo, Z. (2019). Superwetting Janus Membranes: Focusing on Unidirectional Transport Behaviors and Multiple Applications. J. Mater. Chem. A *7*, 12921–12950. https://doi.org/10.1039/c9ta02682g.
34. Odio, M., and Friedlander, S.F. (2000). Diaper Dermatitis and Advances in Diaper Technology. Curr. Opin. Pediatr. *12*, 342–346. https://doi.org/10.1097/00008480-200008000-00011.
35. Farage, M.A. (2010). Evaluating Lotion Transfer from Products to Skin Using the Behind-the-Knee Test. Skin Res. Technol. *16*, 243–252. https://doi.org/10.1111/J.1600-0846.2010.00430.X.
36. Padmavathy, N., and Vijayaraghavan, R. (2008). Enhanced Bioactivity of ZnO Nanoparticles—an Antimicrobial Study. Sci. Technol. Adv. Mater. *9*, 35004–35011. https://doi.org/10.1088/1468-6996/9/3/035004.
37. Pereira, A.P.d.S., Silva, M.H.P.d., Lima Júnior, É.P., Paula, A.d.S., and Tommasini, F.J. (2017). Processing and Characterization of PET Composites Reinforced with Geopolymer Concrete Waste. Mat. Res. *20*, 411–420. https://doi.org/10.1590/1980-5373-MR-2017-0734.
38. Parvinzadeh, M., and Ebrahimi, I. (2011). Influence of Atmospheric-Air Plasma on the Coating of a Nonionic Lubricating Agent on Polyester Fiber. Radiat. Eff. Defect Solid *166*, 408–416. https://doi.org/10.1080/10420150.2011.553230.
39. Bhattacharya, S., Chaudhari, S.B., Bhattacharya, S., and Chaudhari, S. (2014). Study on Structural, Mechanical and Functional Properties of Polyester Silica Nanocomposite Fabric. Int. J. Pure Appl. Sci. Technol. *21*, 43–52.
40. Johnson, L.M., Gao, L., Shields IV, C.W., Smith, M., Efimenko, K., Cushing, K., Genzer, J., and López, G.P. (2013). Elastomeric Microparticles for Acoustic Mediated Bioseparations. J. Nanobiotechnology *11*, 22. https://doi.org/10.1186/1477-3155-11-22.
41. Silva, F.A.B., Chagas-Silva, F.A., Florenzano, F.H., and Pissetti, F.L. (2016). Poly(Dimethylsiloxane) and Poly [Vinyltrimethoxysilane-Co-2-(Dimethylamino) Ethyl Methacrylate] Based Cross-Linked Oroganic-Inorganic Hybrid Adsorbent for Copper(II) Removal from Aqueous Solutions. J. Braz. Chem. Soc. *27*, 2181–2191. https://doi.org/10.5935/0103-5053.20160110.
42. Parada, M., Zhou, X., Derome, D., Rossi, R.M., and Carmeliet, J. (2018). Modeling Wicking in Textiles Using the Dual Porosity Approach. Textil. Res. J. *89*, 3519–3528. https://doi.org/10.1177/0040517518758007.
43. Parada, M., Vontobel, P., Rossi, R.M., Derome, D., and Carmeliet, J. (2017). Dynamic Wicking Process in Textiles. Transp. Porous Media *119*, 611–632. https://doi.org/10.1007/S11242-017-0901-5/TABLES/3.
44. Lei, M., Li, Y., Liu, Y., Ma, Y., Cheng, L., and Hu, Y. (2020). Effect of Weaving Structures on the Water Wicking–Evaporating Behavior of Woven Fabrics. Polymers *12*, 422. https://doi.org/10.3390/POLYM12020422.
45. Bajpayee, A., Rivera-Gonzalez, N., Braham, E.J., Alivio, T.E.G., Anita, Alvi, S., Alvi, S., Li, C., Cool, N., Al-Hashimi, M., et al. (2022). Multiscale Textured Mesh Substrates That Glide Alcohol Droplets and Impede Ice Nucleation. Adv. Eng. Mater. *24*, 2101524. https://doi.org/10.1002/ADEM.202101524.
46. Johnson, C.L., and Dunn, A.C. (2019). Wear Mode Control of Polydimethylsiloxane (PDMS) by Load and Composition. Wear *438–439*, 203066. https://doi.org/10.1016/J.WEAR.2019.203066.
47. He, B., Chen, W., and Jane Wang, Q. (2008). Surface Texture Effect on Friction of a Microtextured Poly(Dimethylsiloxane) (PDMS). Tribol. Lett. *31*, 187–197. https://doi.org/10.1007/S11249-008-9351-0/FIGURES/16.
48. Lee, S.J., Kim, G.M., and Kim, C.L. (2021). Effect of Glass Bubbles on Friction and Wear Characteristics of PDMS-Based Composites. Coatings *11*, 603. https://doi.org/10.3390/COATINGS11050603.
49. Salamonsen, L.A. (2021). Menstrual Fluid Factors Mediate Endometrial Repair. Front. Reprod. Health *3*, 779979. https://doi.org/10.3389/frph.2021.779979.
50. Farage, M.A., and Maibach, H.I. (1985). The Vulva : Anatomy, Physiology, and Pathology (Informa Healthcare (CRC Press)).
51. Fraser, I.S., McCarron, G., Markham, R., and Resta, R. (2021). Blood and Total Fluid Content of Menstrual Discharge. Obstet. Gynecol. *65*, 194–198. https://doi.org/10.3389/frph.2021.779979.
52. Rees, M.C., Cederholm-Williams, S.A., and Turnbull, A.C. (1985). Coagulation Factors and Fibrinolytic Proteins in Menstrual Fluid Collected from Normal and Menorrhagic Women. BJOG *92*, 1164–1168. https://doi.org/10.1111/j.1471-0528.1985.tb03031.x.
53. Hood, H.H., Spears, J.M., and Worely, J.W. (2010). Menstrual Fluid Simulant Containing Blood Product, Gelatin Polyacrimde and Buffer. US *7*, 659. 372 B2.

STAR★METHODS

KEY RESOURCES TABLE

REAGENT or RESOURCE	SOURCE	IDENTIFIER
Chemicals, peptides, and recombinant proteins		
Zinc Metal	McMaster0Carr	1007T171
Polydimethylsiloxane (Sylgard 184™)	DOW Chemical	
HPLC grade Toluene	Fisher Chemical ACS	108-88-3
Simulant menses	Biochemazone™	Cat#BZ266
Other		
100% Polyester Mosquito Netting	Hobby Lobby	Cat#2132793
100% Cotton Fabric	JOANN Fabric and Craft Store	Cat#1914-0862
100% Polyester Gabardine fabric	JOANN Fabric and Craft Store	Cat#1673-4832
100% Polyester Knit Fabric	JOANN Fabric and Craft Store	Cat#1740-3114
100% Polyester Fleece Fabric	JOANN Fabric and Craft Store	Cat#2618-0556
90% Polyester 10% Spandex Double Brushed Jersey Knit Fabric	JOANN Fabric and Craft Store	Cat#1792-1453
100% Polyester Lining Fabric	JOANN Fabric and Craft Store	Cat#73-1927

RESOURCE AVAILABILITY

Lead contact

Further information and requests for resources and reagents should be directed to and will be fulfilled by the lead contact, Sarbajit Banerjee (banerjee@chem.tamu.edu)

Materials availability

This study did not generate new unique reagents.

Data and code availability

- All data reported in this paper will be shared by the lead contact upon request.
- This paper does not report original code.
- Any additional information required to reanalyze the data reported in this paper is available from the lead contact upon request.

METHOD DETAILS

Materials

Reagents and their commercial sources are as follows: Zinc Metal 99%, 200 μm thickness (McMaster-Carr); 100% polyester mosquito netting (Hobby Lobby); 100% cotton (JOANN Fabric and Craft Store); 100% polyester Gabardine (JOANN Fabric and Craft Store); 100% polyester fleece fabric (JOANN Fabric and Craft Store); 90% polyester, 10% spandex double brushed jersey knit fabric (JOANN Fabric and Craft Store), 100% polyester lining fabric (JOANN Fabric and Craft Store); polydimethylsiloxane (PDMS, Sylgard 184™ Silicone Elastomer Dow Chemical); HPLC grade toluene (Fisher Chemical ACS);. Simulated Menstrual Fluid (BiochemazoneTM). All chemicals and solvents were used as received.

ZnO synthesis

ZnO tetrapods (ZnO-t) were synthesized by modifying a previously reported procedure.14,16,18 Zinc strips were cut into 5 mm × 5 mm squares and placed within a 316 stainless steel mesh (80×80 gauge, McMaster-Carr) boat (with lateral dimensions of 25 cm × 5 cm) in a thin layer. The boat was then placed at the center of a quartz tube (7.62 cm in diameter, and 121.92 cm length), which was inserted within a single-zone tube furnace (Thermo Scientific Linderbergy/Blue M™ with a maximum achievable temperature of 1100°C). The tube was heated in a static air ambient to 950 °C at a rate of 43 °C/min. Once nucleation of the ZnO-t was initiated, the furnace was allowed to continue heating for approximately 3–5 min and air was gently circulated through the tube using a 22.86 cm portable personal fan with two speeds (Walmart) at periodic intervals until flow of ZnO-t particles was no longer observed. The flow of air periodically allows for nucleation of the tetrapods to occur until all zinc pieces have reacted. Next, the furnace was turned off and allowed to cool to room temperature; air was

circulated until no additional product was seen to form. Once the tube and boat were removed from the furnace, approximately 10–14 g of ZnO-t were collected that appeared to be a white/light gray/cream color, very fluffy and soft in texture.

Fabric functionalization

A 7.62 cm × 7.62 cm 100% polyester mosquito netting (Hobby Lobby, _thickness, _pore size) was suspended in air and coated with a mixture of 150, 300, 600, or 1200 mg of ZnO-t, as specified in text, dispersed in 15 mL of 10 wt.% polydimethylsiloxane (PDMS, Sylgard 184™ Silicone Elastomer Dow Chemical) in toluene on a single side. This results in an intended loading of 2.58, 5.17, 10.33, and 20.67 mg/cm^2 ZnO-t respectively. PDMS solutions were generated by mixing 10 wt.% elastomer base in 200 mL toluene (Fisher Chemical ACS and HPLC grade, comprising 89 wt.% of the final polymer solution) and stirring for 30 minutes. Curing agent (comprising the remaining 1 wt.%) was then added and the solution was stirred for one additional 4 hours. All coating with the PDMS were generated with the same 260 μL/cm2 of 10 wt.% PDMDS solution. Upon addition of ZnO-t to the 10% PDMS solution, the mixture was agitated for 30 s in a sonicator before being sprayed onto the fabric using a 0.3 mm airbrush nozzle (Master) attached to an air compressor with an output pressure of 35 kPa. The substrate was then cured at 100°C for 35 min while remaining suspended in air. The lower, impermeable layer fabric was functionalized in the same manner onto a densely woven fabric instead of the porous mosquito netting in order to generate the impermeable barrier, rather than allowing for unidirectional flow. Either a 100% cotton or a 100% polyester fabric was used in place of the mosquito netting and a mixture of 600 mg ZnO-t suspended in 15 mL 10 wt. % PDMS in toluene was applied via spray coating while the fabric was suspended. The lower layer fabrics were similarly cured at 100°C for 35 min while remaining suspended in air.

Coating characterization

The morphology of the coatings was examined using scanning electron microscopy (SEM) (JEOL JSM-7500F). The following parameters were used: emission current of 20 μA, probe current of 8 μA, accelerating voltage of 5 kV, and a 15 mm working distance. Substrates were cut into 0.5 cm × 0.5 cm samples and mounted on aluminum holders using double-sided carbon tape prior to being coated with 5 nm of Pt using a 208HR High-Resolution Sputter Coater. Energy dispersive X-ray spectroscopy (EDX) measurements were recorded using an Oxford system using the following parameters: accelerating voltage of 10 kV, emission current of 20 μA, probe current of 12 μA, and working distance of 8 mm. A video microscope (Jiusion Digital Microscope) was used to obtain macroscopic images of the fabric.

A Bruker Vertex-70 with PIKE MIRacle single-reflection horizontal attenuated total reflectance (ATR) accessory was used to collect Fourier-transform infrared (FTIR) spectroscopy data. Wettability of the coated substrates was evaluated by measuring contact angles using a cell phone equipped with a 0.62 X wide lens (Selvim). The values reported are an average of a minimum of measurements taken across three distinct areas across the substrate. Water droplets of approximately 7 μL were manually placed on the substrate. For each instance, a digital photograph was captured and analyzed using ImageJ. Contact angles and wettability were evaluated with deionized water (ρ = 18.2 MΩ·cm-1).

Performance and durability evaluation: middle layer absorption capacity

To select an absorbent middle layer a variety of fabrics were evaluated. Each one was cut to 5 x 7.5 cm and 2 mL of water was allowed to absorb into the fabrics. The fabrics were then lifted to see if any water remained unabsorbed. For each type of fabric, the number of layers of fabric was then increased and new samples were evaluated until the 2 mL water were absorbed without leaving any residual residue when lifted. Fabrics were then selected based on the number of layers required to absorb the water, how effectively the fabric distributed the water longitudinally resulting in a drier feeling fabric post testing, the thickness of the resulting stack of fabric, and then the softness and flexibility of the fabric. Two layers of a double brushed 100% polyester fabric of 1.61 mm thickness resulting in a total thickness of approximately _ for the stack was chosen. Evaluation of the effectiveness of adding an additional layer of superhydrophilic 100% polyester liner between the two layers of absorbent middle layers and the body facing functionalized mosquito netting on lowering the strike-through times was additionally evaluated.

Performance and durability evaluation: repeated liquid strike-through time

Guided by the ISO-9073-13 standard,42 the repeated liquid strike-through time of the Janus functionalized mosquito netting membrane was performed. The standard was scaled from the original 125 mm × 125 mm sample size to a smaller 5 cm × 7.5 cm sample to allow for a direct comparison of products developed to commercially available options. A strike-through plate was a machined acrylic plate made to mimic the specification of the standard for the smaller sample size, as shown in Figure S7. A top base plate was added to the top of the strike-through plate to increase the weight of the acrylic plate to 129 g, as shown in Figure S8. Tight-tolerance multipurpose 304 stainless steel wire (McMaster Carr, 4.23 mm diameter) was interfaced with the strike-through plate serving as electrode leads which were connected to a circuit which was closed in the presence of the saline solution illuminating a blue LED light bulb. The strike-through time was defined as the time it took for the light bulb to illuminate then fully turn off which was monitored by video recording, as shown in Video S1. The amount of liquid used for each strike-through time was also scaled back to 1.2 mL dispensed three times per sample to provide the same volume per area as required by the standard but adjusted for the smaller sample size. Fabric was used in place of the filter paper as the absorbent pad to mimic real world use and allow for testing of fully assembled devices. The average flow rate of the funnel used was 25 mL in 3.5 ± 0.25 s as per the standard,

however it did not possess a magnetic exit valve, so the time of the liquid being dispensed was not used as the metric for the time at which the strike-through time should begin. A baseplate was also not used as the laboratory benchtop served this purpose effectively.

For a typical strike-through test of Janus membrane, a ZnO-t/PDMS functionalized mosquito net was placed on top of two layers of 100% polyester absorbent filler and the strike-through plate was placed on top with the acrylic side facing down and the leads attached to the circuit fitted with the indicator LED. Three aliquots of 1.2 mL saline solution (0.9 wt.% NaCl) were prepared. A video recording focusing on the LED bulb was started and the first aliquot of saline solution was poured through the funnel into the strike plate, illuminating the LED. After the light bulb went out, a one-minute timer was begun to allow the solution to fully saturate into the filler material through the Janus membrane. This was repeated two additional times. The strike plate was then removed, and wetback testing was performed.

Performance and durability evaluation: wetback test

Following the repeated liquid strike-through test, a wetback test was used to determine the ability of the functionalized fabrics to resist the transportation of the already permeated liquid back towards the body after absorption. This test was guided by the ISO-9073-14,13 but followed similar deviations as discussed above for the liquid strike-through test to accommodate testing of full products, as shown in the setup in Figure S9. Following three repeated liquid strike-through tests, resulting in a total of 3.60 mL saline solution being deposited onto the menstrual pad test sample, the strike-through plate was removed from the menstrual pad test sample, and a 'simulated baby weight', as described by the standard was placed on top of the sample for three minutes. The size of the simulated baby weight was scaled down to accommodate the reduced size of the test samples to ensure a similar pressure per area was applied as the standard specifies. The side of the simulated baby weight that was placed on the menstrual care product was 4 x 6.5 cm, and the height was 5 cm. This resulted in a total weight of 1031 g. Polyurethane foam (19.05 mm thick, Super Cushioning, McMaster Carr) was cut to 4 x 6.5 cm and attached to the simulated baby weight on the side that interfaces with the menstrual care products to provide a cushion when the weight is placed. The foam was first covered in a layer of polyethylene drop cloth film (25 μm thickness, Nanja) secured using masking tape on the sides.

The simulated baby weight was allowed to sit on the samples for three minutes to ensure all liquid was distributed throughout the pad prior to wetback measurement. The simulated baby weight was then removed, and the foam side was wiped to ensure that excess liquid was removed. Two pieces pre-weighed filter paper (7.5 cm, VWR) were then placed on the menstrual care product sample to serve as the pick up paper specified by the standard. The simulated baby weight was then placed gently onto the pick up paper and allowed to sit for two minutes. The pick up paper was then weighed to determine the amount of water that was absorbed during exposure to the saturated pads.

In order to test the extent to which the lower, impermeable layer provided leak-proof protection, the wetback test was evaluated after performing the strike-through test on the two layers of the absorbent 100% polyester filler fabric. The cloth-facing fabric was then placed on top of the saturated absorbent filler layers with the functionalized side facing the saline saturated filler fabric layers. The simulated baby weight was then allowed to sit on top of this assembly for three minutes. The simulated baby weight was then removed, any excess liquid was wiped, and the pick up papers were then placed on top of the uncoated side of the cloth-facing layer The simulated baby weight was then placed back on top of this assembly and allowed to sit for two minutes. The pre-weighed pick up paper was then removed and weighed as before to determine how much saline solution had been absorbed. Strike-through and wetback testing were repeated five times per sample for three separate samples, generating a total of fifteen trials, for each of the ZnO-t/PDMS mosquito netting Janus membranes and the ZnO-t/PDMS clothes facing backing layers. The filler material was replaced each time between trials. Single use and reusable commercial products were similarly tested a total of fifteen times, using a new sample each time. The single use commercial products were cut to 5 x 7.5 cm to allow for a more direct comparison of the product thickness relation to wetback capacity across commercial and newly designed samples.

Performance and durability evaluation: menstrual fluid simulant

Strike-through and wetback performance testing was performed with menstrual fluid simulant (Biochemazone, BZ266). were repeated five connective times with the same methods described above for the saline solution.

Performance and durability evaluation: washability

Durability of Janus membrane samples created by coating 100% polyester mosquito netting cut to 7.62 cm x 7.62 cm with 10.33 mg/cm^2 ZnO-t with PDMS on one side towards hand washing and machine washing was evaluated. Samples were cut to 2 x 2 cm. One membrane was washed in a conventional washing machine on a regular cycle within a fine mesh laundry bag to prevent loss of the sample within the machine. 10 mL Tide laundry detergent was included prior to the wash cycle being started. A separate sample was washed by hand by including 1 L of water and 1 g of Tide laundry detergent in a 2 L capacity cylindrical jar with a lid. The jar was sealed and shaken thirty times and allowed to sit for 10 minutes. The sample was then rinsed with water and allowed to dry. This was repeated five times. Samples were analyzed by SEM and contact angles were measured on washed samples.

Surface tension testing of simulated menstrual fluids

The surface tension of the simulated menstrual fluid was measured with an optical goniometer (Attention Theta Lite). The measurements were acquired three times for 4.00 μL volumes with a drop-out rate of 2.00 μL/s.